Article:
(2017) Persistence of the Z=28 Shell Gap Around Ni 78: First Spectroscopy of Cu 79. Physical Review Letters. 192501. ISSN: 1079-7114

https://doi.org/10.1103/PhysRevLett.119.192501

Persistence of the $Z = 28$ Shell Gap Around ^{78}Ni: First Spectroscopy of ^{79}Cu

L. Olivier,[1] S. Franchoo,[1] M. Niikura,[2] Z. Vajta,[3] D. Sohler,[3] P. Doornenbal,[4] A. Obertelli,[5,4] Y. Tsunoda,[6] T. Otsuka,[2,4,6] G. Authelet,[5] H. Baba,[4] D. Calvet,[5] F. Château,[5] A. Corsi,[5] A. Delbart,[5] J.-M. Gheller,[5] A. Gillibert,[5] T. Isobe,[4] V. Lapoux,[5] M. Matsushita,[7] S. Momiyama,[2] T. Motobayashi,[4] H. Otsu,[4] C. Péron,[5] A. Peyaud,[5] E. C. Pollacco,[5] J.-Y. Roussé,[5] H. Sakurai,[2,4] C. Santamaria,[5,4] M. Sasano,[4] Y. Shiga,[4,8] S. Takeuchi,[4] R. Taniuchi,[2,4] T. Uesaka,[4] H. Wang,[4] K. Yoneda,[4] F. Browne,[9] L. X. Chung,[10] Z. Dombradi,[3] F. Flavigny,[1] F. Giacoppo,[11,*] A. Gottardo,[1] K. Hadyńska-Klęk,[11] Z. Korkulu,[3] S. Koyama,[2] Y. Kubota,[4,7] J. Lee,[12] M. Lettmann,[13] C. Louchart,[13] R. Lozeva,[14,†] K. Matsui,[2,4] T. Miyazaki,[2] S. Nishimura,[4] K. Ogata,[15] S. Ota,[7] Z. Patel,[16] E. Sahin,[11] C. Shand,[16] P.-A. Söderström,[4] I. Stefan,[1] D. Steppenbeck,[7] T. Sumikama,[17] D. Suzuki,[1] V. Werner,[13] J. Wu,[4,18] and Z. Xu[12]

[1]*Institut de Physique Nucléaire, IN2P3-CNRS, Université Paris-Sud, Université Paris-Saclay, 91406 Orsay Cedex, France*
[2]*Department of Physics, University of Tokyo, 7-3-1 Hongo, Bunkyo, Tokyo 113-0033, Japan*
[3]*MTA Atomki, P.O. Box 51, Debrecen H-4001, Hungary*
[4]*RIKEN Nishina Center, 2-1 Hirosawa, Wako, Saitama 351-0198, Japan*
[5]*IRFU, CEA, Université Paris-Saclay, F-91191 Gif-sur-Yvette, France*
[6]*Center for Nuclear Study, University of Tokyo, 7-3-1 Hongo, Bunkyo, Tokyo 113-0033, Japan*
[7]*Center for Nuclear Study, University of Tokyo, RIKEN campus, Wako, Saitama 351-0198, Japan*
[8]*Department of Physics, Rikkyo University, 3-34-1 Nishi-Ikebukuro, Toshima, Tokyo 172-8501, Japan*
[9]*School of Computing Engineering and Mathematics, University of Brighton, Brighton BN2 4GJ, United Kingdom*
[10]*Institute for Nuclear Science & Technology, VINATOM, P.O. Box 5T-160, Nghia Do, Hanoi, Vietnam*
[11]*Department of Physics, University of Oslo, N-0316 Oslo, Norway*
[12]*Department of Physics, The University of Hong Kong, Pokfulam, Hong Kong*
[13]*Institut für Kernphysik, Technische Universität Darmstadt, 64289 Darmstadt, Germany*
[15]*IPHC, CNRS/IN2P3, Université de Strasbourg, F-67037 Strasbourg, France*
[15]*Research Center for Nuclear Physics (RCNP), Osaka University, Ibaraki 567-0047, Japan*
[16]*Department of Physics, University of Surrey, Guildford GU2 7XH, United Kingdom*
[17]*Department of Physics, Tohoku University, Sendai 980-8578, Japan*
[18]*State Key Laboratory of Nuclear Physics and Technology, Peking University, Beijing 100871, People's Republic of China*

(Received 1 February 2017; revised manuscript received 20 September 2017; published 6 November 2017)

In-beam γ-ray spectroscopy of ^{79}Cu is performed at the Radioactive Isotope Beam Factory of RIKEN. The nucleus of interest is produced through proton knockout from a ^{80}Zn beam at 270 MeV/nucleon. The level scheme up to 4.6 MeV is established for the first time and the results are compared to Monte Carlo shell-model calculations. We do not observe significant knockout feeding to the excited states below 2.2 MeV, which indicates that the $Z = 28$ gap at $N = 50$ remains large. The results show that the ^{79}Cu nucleus can be described in terms of a valence proton outside a ^{78}Ni core, implying the magic character of the latter.

DOI: 10.1103/PhysRevLett.119.192501

The shell model constitutes one of the main building blocks of our understanding of nuclear structure. Its robustness is well proven for nuclei close to the valley of stability, where it successfully predicts and explains the occurrence of magic numbers [1,2]. However, these magic numbers are not universal throughout the nuclear chart and their evolution far from stability, observed experimentally over the last decades, has generated much interest [3]. For example, the magic numbers $N = 20$ and 28 may disappear [4–7] while new magic numbers arise at $N = 14$, 16 and 32, 34, respectively [8–13]. Although shell gaps, defined within a given theoretical framework as differences of effective single-particle energies (ESPE), are not observables [14], they are useful quantities to assess the underlying structure of nuclei [15–17]. The nuclear potential acting on nuclei far from stability can induce drifts of the single-particle orbitals and their behavior as a function of isospin can be understood within the shell model [18–22]. Difficulties arise, however, when the single-particle properties are masked by correlations that stem from residual interactions and discriminating between the two effects is nontrivial.

In the shell model as it was initially formulated, the proton $\pi f_{7/2}$ orbital separates from the $3\hbar\omega$ harmonic oscillator shell because of the spin-orbit splitting and forms the $Z = 28$ gap. The neutron $\nu g_{9/2}$ orbital splits off from the $4\hbar\omega$ shell to join the $3\hbar\omega$ orbits and creates a magic number at $N = 50$. With 28 protons and 50 neutrons, the ^{78}Ni nucleus is thus expected to be one of the most neutron-rich doubly magic nuclei, making it of great interest for nuclear structure. Up to now, no evidence has been found for the disappearance of the shell closures at $Z = 28$

and $N = 50$, even if recent studies hint at a possible weakening of the $N=50$ magic number below ^{78}Ni [23,24]. On the contrary, the half-life of ^{78}Ni was determined at 122.2(5.1) ms, suggesting a survival of magicity [25], and calculations predict a first excited state in ^{78}Ni above 2 MeV [24,26–28]. But so far no other information about ^{78}Ni is available, with the exception of indirect ones such as the mass of ^{79}Cu, measured recently [29].

The size of the $Z = 28$ gap might be affected by a drift of the single-particle energies. When adding neutrons in the $\nu g_{9/2}$ orbital above the $N = 40$ subshell gap, there is a sudden decrease of the energy of the first $5/2^-$ excited state relative to the $3/2^-$ ground state in ^{71,73}Cu, which was established from β decay [30]. The subsequent inversion of these two states in ^{75}Cu was evidenced from collinear laser spectroscopy [31]. Theoretically, these $3/2^-$ and $5/2^-$ levels are linked through the main components in their respective wave functions with the $p_{3/2}$ and $f_{5/2}$ proton single-particle states [18,32,33].

The behavior of the $\pi f_{7/2}$ spin-orbit partner is more difficult to determine. This orbital is of primary importance as it is one of the two orbitals defining the $Z = 28$ gap. Access to this hole state is possible through proton transfer or knockout reactions [34]. While spectroscopic factors extracted in proton pickup reactions allow in principle for the measurement of strength functions, it is a challenge to identify the smallest components or those that are situated at high excitation energy. Moreover, away from the valley of stability, the resort to inverse kinematics with radioactive ion beams limits the count rate as well as the resolution that can be achieved. Today, data are available for the ^{70}Zn$(d,{}^3$He$)^{69}$Cu [35,36] and ^{72}Zn$(d,{}^3$He$)^{71}$Cu [37] reactions, on both sides of the $N = 40$ subshell gap. The measured part of the $\pi f_{7/2}^{-1}$ centroid was seen to remain at 3.8 MeV in ^{71}Cu, compared to a lower limit of 2.45 MeV in ^{69}Cu. While it is not possible to clarify in what direction or to what extent the energy of the centroid shifts, it remains sufficiently high and the $Z = 28$ gap does not appear to be appreciably affected.

In this Letter we report on our measurement of the proton knockout of ^{80}Zn into ^{79}Cu, at $N = 50$. The reaction mechanism favors proton hole states, including the $\pi f_{7/2}^{-1}$ one. It sheds the first light on the evolution of nuclear structure in the most neutron-rich copper isotopes available today, in the close vicinity of ^{78}Ni.

The experiment was performed at the Radioactive Isotope Beam Factory (RIBF), operated jointly by the RIKEN Nishina Center and the Center for Nuclear Study of the University of Tokyo. A ^{238}U beam with an energy of 345 MeV per nucleon and an average intensity of 12 pnA was sent on a 3-mm thick ^{9}Be target for in-flight fission. The secondary ^{80}Zn beam was selected in the BigRIPS separator [38]. A secondary target was placed at the end of BigRIPS. The isotopes before and after the secondary target were identified on an event-by-event basis in the BigRIPS and ZeroDegree spectrometers, respectively, with the TOF-$B\rho$-ΔE method [39]. The average ^{80}Zn intensity was 260 particles per second. The detector setup installed between the two spectrometers was composed of the MINOS device [40] mounted inside the DALI2 γ-ray multidetector [41]. MINOS consists of a liquid-hydrogen target surrounded by a cylindrical time-projection chamber (TPC). The target was 102(1) mm long with a density of 70.97 kg/m^3. The energy of the isotopes was 270 and 180 MeV per nucleon at the entrance and exit of MINOS, respectively. The ^{79}Cu nucleus was produced mainly through proton knockout from the incoming ^{80}Zn isotopes, the $(p,3p)$ channel from ^{81}Ga contributing to only 8%. The emitted protons were tracked in the TPC, while the beam trajectory was given by two parallel-plate avalanche counters [42] before the target. For the events with at least one proton detected in the TPC, this ensured the reconstruction of the interaction-vertex position with 95% efficiency and a 5-mm uncertainty (full width at half maximum) along the beam axis. The DALI2 array consists of 186 NaI scintillator crystals that were calibrated with ^{60}Co, ^{137}Cs, and ^{88}Y sources. When several crystals separated by no more than 15 cm were hit by γ rays, the energies were summed before Doppler correction and the event was considered as one single γ ray, a method known as add back. The photopeak

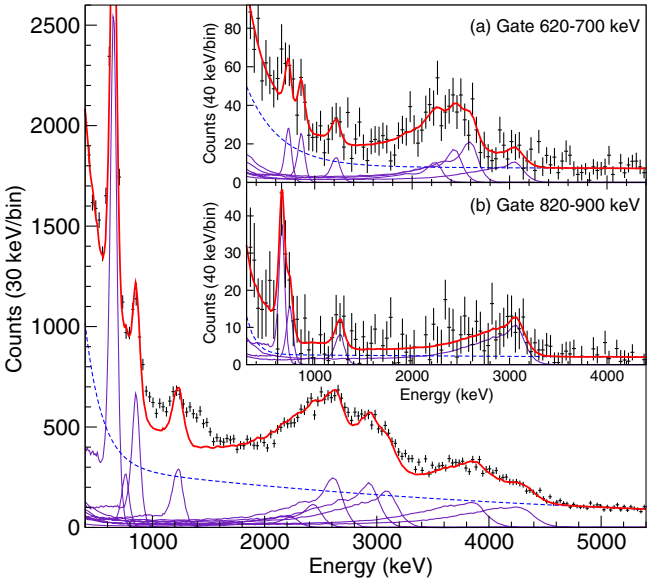

FIG. 1. γ-ray spectrum of ^{80}Zn$(p,2p)^{79}$Cu after Doppler correction, with multiplicities below 4. The experimental data points are in black, with the double-exponential background as the blue dashed line, the simulated response function of each transition in purple, and the sum of the simulated response functions with the background in red. Discrepancies between the data and the fit are due to nonidentified transitions (see text). The inset shows γ-γ coincidences after background subtraction for a gate set on the 656-keV [subpanel (a)] and 855-keV [subpanel (b)] transitions.

detection efficiency with add back was 27% and the energy resolution was $\sigma = 45$ keV for a 1 MeV transition emitted in flight at 250 MeV per nucleon.

The γ-ray spectrum obtained for ^{80}Zn$(p, 2p)^{79}$Cu after Doppler correction is shown in Fig. 1. Two clear transitions were found at 656(5) and 855(6) keV, while three structures were seen in the ranges 1.0–1.5 MeV, 2.0–3.4 MeV, and 3.4–4.5 MeV. γ-γ coincidences with background subtraction were performed, gating on the 656- and 855-keV transitions. The corresponding coincidence spectra are shown in the insets of Fig. 1. Seven transitions are observed when a gate is set around 656 keV: 750(20), 860(10), 1220(30), 2240(40), 2440(40), 2600(40), and 3070(30) keV. When a gate is set around 855 keV, peaks at 660(20), 760(30), 1250(30), and 3050(30) keV are seen. Three other γ rays were found at 2940(60), 3880(40), and 4300(40) keV with no coincidence with any other transition. All transitions observed are listed in Table I. The uncertainties on the energies were obtained by adding quadratically calibration (5 keV) and statistical uncertainties.

The response functions of DALI2 for all transitions were obtained from Geant4 simulations [43], taking into account the measured intrinsic resolution of each crystal. While the simulated efficiency agreed within 5% with measurements made with sources and solid targets in previous experiments, we allowed for a larger margin of 10% to account for the thick liquid target that was used here. The ^{79}Cu spectrum was fitted with these response functions as well as with a background composed of two exponential functions, as shown in Fig. 1, in order to obtain the intensity of each transition. The structure between 3.4 and 4.5 MeV is well fitted, while discrepancies are observed for the two other structures, mainly between 1.0 and 1.5 MeV. This indicates that other transitions are present in the spectrum. The uncertainties on the intensities in Table I have been estimated by taking into account these discrepancies.

TABLE I. Transitions seen in the ^{80}Zn$(p, 2p)^{79}$Cu spectrum. Intensities are normalized with respect to the intensity of the 656-keV transition, and take into account all multiplicities.

Energy (keV)	Intensity (relative)
656(5)[b]	100(11)
750(20)[a,b]	9(2)
855(6)[a]	33(4)
1220(30)[a,b]	16(4)
2240(40)[a]	4(2)
2440(40)[a]	21(3)
2600(40)[a]	40(7)
2940(60)	33(6)
3070(30)[a,b]	28(6)
3880(40)	34(4)
4300(40)	31(4)

[a]Transitions observed in the γ-γ spectrum when gating on the 656-keV transition.
[b]Transitions observed in the γ-γ spectrum when gating on the 855-keV transition.

The level scheme for ^{79}Cu, based on the intensities of the transitions and the γ-γ coincidences, is shown in Fig. 2. Considering the intensities of the 656- and 855-keV transitions, the latter is placed on top of the former. No γ transition was seen below 656 keV, while it was possible elsewhere in the data set to detect peaks down to 200 keV. We place the first excited state of ^{79}Cu at 656(5) keV and the second one at 1511(8) keV. A direct decay of the 1511-keV level to the ground state cannot be excluded but has not been observed: by fitting the spectrum, a limit can be put that is equal to one third of the intensity of the 855-keV transition. The 750-, 1220-, and 3070-keV transitions, found in coincidence with both the 656- and 855-keV ones, are placed on top of the 1511-keV level. This gives three levels at 2260(20), 2730(30), and 4580(30) keV, respectively. The 2260- and 2730-keV levels are shown as dashed lines because we cannot exclude the coincidence of the 750- and 1220-keV transitions with other γ rays due to low statistics.

No information about the half-lives of levels was available and therefore we considered all decays to be prompt. A half-life of several tens of picoseconds could change the energy by a few percent, but it would not affect the placement of the transitions in the scheme. For example, a 100 ps half-life corresponds to an offset of 24 keV for a 656-keV transition.

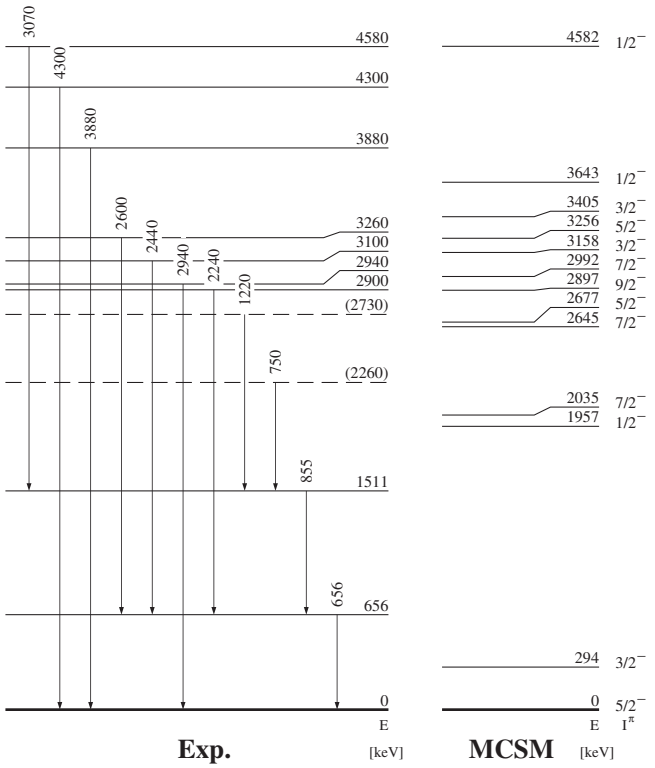

FIG. 2. Proposed level scheme for ^{79}Cu. The experimental results (left) are compared to Monte Carlo shell-model (MCSM) calculations (right).

TABLE II. Occupation numbers of proton orbits and spectroscopic factors (SF) for the lowest and the three first $7/2^-$ calculated states in ^{79}Cu, as well as for the ground state of ^{80}Zn.

	E (MeV)	J^π	$f_{7/2}$	$f_{5/2}$	$p_{3/2}$	$p_{1/2}$	$g_{9/2}$	$d_{5/2}$	SF
^{79}Cu	0	$5/2^-$	7.73	1.05	0.15	0.02	0.03	0.01	1.33
	0.294	$3/2^-$	7.73	0.17	1.02	0.03	0.04	0.01	0.57
	1.957	$1/2^-$	7.57	0.48	0.29	0.62	0.03	0.01	0.04
	2.035	$7/2^-$	6.82	1.49	0.57	0.04	0.07	0.01	5.58
	2.645	$7/2^-$	7.22	1.09	0.61	0.03	0.04	0.01	0.15
	2.992	$7/2^-$	7.54	1.00	0.37	0.05	0.03	0.00	0.43
^{80}Zn	0	0^+	7.66	1.43	0.73	0.06	0.10	0.01	—

Monte Carlo shell-model (MCSM) calculations were carried out in the $pfg_{9/2}d_{5/2}$ model space of protons and neutrons with an A3DA Hamiltonian [27]. Previous results are reproduced within this theoretical framework, like the structure of ^{80,82}Zn [44] and ^{77}Cu [45]. Calculated occupation numbers of proton orbits for the wave functions of the ground state of ^{80}Zn as well as for the lowest calculated states in ^{79}Cu are given in Table II. Spectroscopic factors, corresponding to the overlap between the initial (^{80}Zn) and final (^{79}Cu) wave functions, are also given. The ground state of ^{80}Zn is characterized by a proton component that is distributed over the $\pi f_{5/2}$ and $\pi p_{3/2}$ orbitals. The unpaired proton in ^{79}Cu, after one-proton removal from ^{80}Zn, is expected to reside mainly in the pf orbitals and therefore generates negative-parity final states.

We propose a $5/2^-$ spin for the ground state of ^{79}Cu and a $3/2^-$ spin for the first excited state at 656 keV from the systematics of the copper isotopic chain, as shown in Fig. 3, as well as the systematics of the $N = 50$ isotonic chain above ^{79}Cu [48,49]. The present MCSM calculations support this conclusion. The calculated wave functions for the lowest $5/2^-$ and $3/2^-$ states correspond closely to those of the $\pi f_{5/2}$ (75.3%) and $\pi p_{3/2}$ (74.2%) single-particle states, respectively. From the comparison with ^{77}Cu

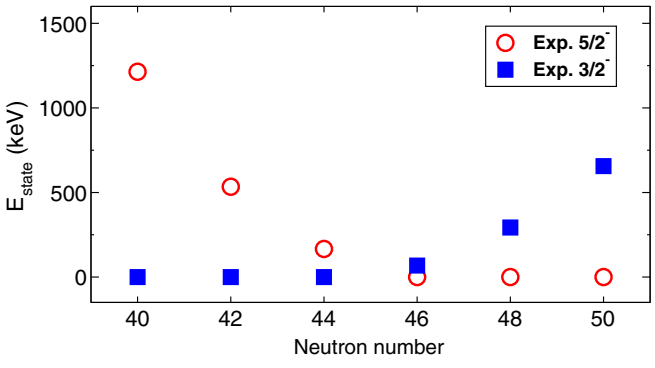

FIG. 3. Systematics of the first $3/2^-$ and $5/2^-$ states in copper isotopes. Data taken from Refs. [30,31,35,45–47] and this work. The error bars are smaller than the data points.

[45,46], the $3/2^-$ level is seen to rise and illustrates the continuation of the inversion of the $\pi p_{3/2}$ and $\pi f_{5/2}$ orbitals that is known from the preceding copper isotopes.

For the second excited state at 1511 keV, the calculation offers two possibilities: a $1/2^-$ state at 1957 keV, with 48.3% $\pi p_{1/2}$ single-particle character, or a $7/2^-$ state at 2035 keV, whose 64.1% of the wave function is built from a $\pi f_{7/2}^{-1}$ hole and two protons in $\pi f_{5/2}p_{3/2}$. The absence of direct feeding in the knockout reaction disfavors the $7/2^-$ assignment, for which the calculated spectroscopic factor is high. Comparing the transition strengths for $1/2^-$ and $7/2^-$ spins obtained from calculated $B(M1)$ and $B(E2)$ values and experimental energies, we find that the ratio $\lambda(1/2_1^- \to 5/2_{gs}^-)/\lambda(1/2_1^- \to 3/2_1^-)$ equals 3.2 while $\lambda(7/2_1^- \to 5/2_{gs}^-)/\lambda(7/2_1^- \to 3/2_1^-)$ is 427, so we would expect the 1511-keV transition to be stronger than the 855-keV one. We do not see a 1511-keV transition to the ground state because of the limited resolution, but we can put an upper limit of 10(2) for its intensity compared to 33(4) for the 855-keV one, namely, a ratio of 0.30(7). This is closer to the expected value for $1/2^-$ than for $7/2^-$. If this level is a $1/2^-$ state, the low ratio of 0.30(7) would rather support a $\pi p_{1/2}$ single-particle nature for this state, unlike the strongly collective $1/2^-$ state seen at low energy in ^{69,71,73,75}Cu [47,50].

The multiplet of states between 2.7 and 3.3 MeV is interpreted as the coupling of a proton in the $\pi f_{5/2}$ or $\pi p_{3/2}$ orbital with the first 2^+ state of ^{78}Ni, in agreement with the present MCSM calculations for which all calculated states shown above 2.6 MeV are core-coupling states. We can therefore estimate the first 2^+ state of ^{78}Ni at about 3 MeV excitation energy, in accordance with the MCSM calculations and other theoretical studies [24,26–28]. Such a 3-MeV 2_1^+ state in ^{78}Ni, compared to 992 keV in ^{76}Ni [51], indicates a good shell closure at $N = 50$.

In the experimental level scheme, we find that the knockout of a proton results in a final nucleus at high excitation energy, populating several configurations. Because of the structure of the wave function of the ^{80}Zn ground state, we may expect the reaction to populate the $\pi f_{7/2}^{-1}f_{5/2}^2$ hole but also the $\pi f_{7/2}^{-1}f_{5/2}p_{3/2}$ and $\pi f_{7/2}^{-1}p_{3/2}^2$ configurations. The $\pi f_{7/2}^{-1}$ single-particle wave function will mix with the $7/2^-$ members of the $\pi(f_{5/2}, p_{3/2}) \otimes 2^+$ multiplets, resulting in a fragmentation of the strength over several levels. We have no evidence for a strongly fed $7/2^-$ state below 2.2 MeV and we conclude on the absence of a significant part of the $\pi f_{7/2}^{-1}$ strength below this energy.

Concerning cross sections, we determined an inclusive cross section of 7.9(4) mb for the ^{80}Zn$(p, 2p)^{79}$Cu reaction, but reliable exclusive cross sections could not be extracted as the feeding ratio of each level could be affected by nonobserved transitions between high-energy levels. Only an upper limit of 3.8(8) mb for the ground state and a small

value of 0.04(29) mb for the first excited state were found, leaving at least 4.1(9) mb that will mainly belong to states that in their wave function contain a hole in the $\pi f_{7/2}$ orbital. Theoretical single-particle cross sections were calculated using the distorted-wave impulse approximation (DWIA) framework [52] and averaged along the thick target, the beam energy decreasing from 270 to 180 MeV per nucleon. The optical potentials for the incoming proton and the outgoing two protons are obtained by a microscopic framework; the Melbourne nucleon-nucleon G-matrix interaction [53] is folded by a nuclear density calculated with the Bohr-Mottelson single-particle potential [54]. For the ground state, the low-lying $\pi p_{3/2}$ state and the knockout of a $f_{7/2}$ proton, we obtained 2.1, 2.6, and 2.3 mb, respectively, and these numbers should be multiplied by the corresponding spectroscopic factors from the MCSM given in Table II. We did not identify a strongly populated $7/2^-$ state; our observation shows more fragmentation of the single-particle strength than predicted. Although this could be partly explained by the existence of unobserved γ rays, it is also possible that a part of the $\pi f_{7/2}^{-1}$ strength lies above the neutron-separation threshold. Somewhat discrepant with the presented shell-model calculations, this main result calls for further experimental and theoretical investigations.

The $Z = 28$ gap corresponds to the $\pi f_{5/2} f_{7/2}$ ESPE splitting, as the $\pi p_{3/2}$ and $\pi f_{5/2}$ orbitals are inverted and the MCSM calculations put it at 4.9 MeV. Experimentally, we found a lower limit of 2.2 MeV for the $\pi f_{7/2}^{-1}$ hole strength. Even if the latter cannot be directly related to the ESPE because of model-dependent correlations, both experiment and theory show that although the orbital content of the $Z = 28$ gap is changing along the copper isotopic chain, its magicity persists. Therefore, ^{79}Cu can be described as a ^{78}Ni core plus a valence proton. This is in line with the depiction of ^{80}Zn as two-proton configurations with a ^{78}Ni core [44].

In conclusion, we performed the first spectroscopy of ^{79}Cu and compared the results with MCSM calculations. These calculations show the restoration of the single-particle nature of the low-lying states, which is supported by the experiment. There is no significant knockout feeding to the excited states below 2.2 MeV, indicating that the $Z = 28$ gap remains large. The ability to describe the ^{79}Cu nucleus as a valence proton outside a ^{78}Ni core presents us with indirect evidence of the magic character of the latter. Spectroscopy and mass measurement of ^{78}Ni are the next steps for a direct proof of its double magicity.

The authors are thankful to the RIBF and BigRIPS teams for the stable operation and high intensity of the uranium primary beam, and production of secondary beams during the experiment. The development of MINOS and the core MINOS team have been supported by the European Research Council through the ERC Grant No. MINOS-258567. A. O. was supported by JSPS long-term fellowship L-13520 from September 2013 to June 2014 at the RIKEN Nishina Center. A. O. deeply thanks the ERC and JSPS for their support. C. S. was supported by the IPA program at the RIKEN Nishina Center. A. O. and C. S. are grateful to the RIKEN Nishina Center for its hospitality. This work was supported by JSPS Grant-in-Aid for a JSPS Research Fellow (No. 268718). The MCSM calculations were performed on the K computer at RIKEN AICS (hp150224, hp160211). This work was supported in part by the HPCI Strategic Program ("The Origin of Matter and the Universe") and the "Priority Issue on Post-K computer" ("Elucidation of the Fundamental Laws and Evolution of the Universe") from MEXT and JICFuS. Z. D. and Z. V. were supported by the GINOP-2.3.3-15-2016-00034 contract. L. X. C. would like to thank MOST for its support. M. L. and V. W. acknowledge the German BMBF with the supporting No. 05P15RDFN1 and No. 05P12RDFN8. We thank N. Paul for her careful reading of the Letter.

*Present address: Helmholtz Institute Mainz, 55099 Mainz, Germany and GSI Helmholtzzentrum für Schwerionenforschung, 64291 Darmstadt, Germany.
†Present address: CSNSM, IN2P3-CNRS, Université Paris-Sud, Université Paris-Saclay, 91406 Orsay Cedex, France.

[1] M. Goeppert-Meyer, Phys. Rev. **75**, 1969 (1949).
[2] O. Haxel, J. H. D. Jensen, and H. E. Suess, Phys. Rev. **75**, 1766 (1949).
[3] O. Sorlin and M.-G. Porquet, Prog. Part. Nucl. Phys. **61**, 602 (2008).
[4] D. Guillemaud-Mueller, C. Detraz, M. Langevin, F. Naulin, M. de Saint-Simon, C. Thibault, F. Touchard, and M. Epherre, Nucl. Phys. **A426**, 37 (1984).
[5] T. Motobayashi *et al.*, Phys. Lett. B **346**, 9 (1995).
[6] C. M. Campbell *et al.*, Phys. Rev. Lett. **97**, 112501 (2006).
[7] B. Bastin *et al.*, Phys. Rev. Lett. **99**, 022503 (2007).
[8] A. Huck, G. Klotz, A. Knipper, C. Miehe, C. Richard-Serre, G. Walter, A. Poves, H. L. Ravn, and G. Marguier, Phys. Rev. C **31**, 2226 (1985).
[9] P. G. Thirolf *et al.*, Phys. Lett. B **485**, 16 (2000).
[10] E. Becheva *et al.*, Phys. Rev. Lett. **96**, 012501 (2006).
[11] A. Gade *et al.*, Phys. Rev. C **74**, 021302(R) (2006).
[12] C. R. Hoffman *et al.*, Phys. Lett. B **672**, 17 (2009).
[13] D. Steppenbeck *et al.*, Nature (London) **502**, 207 (2013).
[14] T. Duguet, H. Hergert, J. D. Holt, and V. Somà, Phys. Rev. C **92**, 034313 (2015).
[15] A. Poves and A. Zuker, Phys. Rep. **70**, 235 (1981).
[16] T. Otsuka, R. Fujimoto, Y. Utsuno, B. A. Brown, M. Honma, and T. Mizusaki, Phys. Rev. Lett. **87**, 082502 (2001).
[17] E. Caurier, G. Martínez-Pinedo, F. Nowacki, A. Poves, and A. P. Zuker, Rev. Mod. Phys. **77**, 427 (2005).

[18] T. Otsuka, T. Suzuki, R. Fujimoto, H. Grawe, and Y. Akaishi, Phys. Rev. Lett. **95**, 232502 (2005).
[19] T. Otsuka, T. Suzuki, M. Honma, Y. Utsuno, N. Tsunoda, K. Tsukiyama, and M. Hjorth-Jensen, Phys. Rev. Lett. **104**, 012501 (2010).
[20] N. A. Smirnova, B. Bally, K. Heyde, F. Nowacki, and K. Sieja, Phys. Lett. B **686**, 109 (2010).
[21] T. Otsuka, Phys. Scr. **T152**, 014007 (2013).
[22] T. Otsuka and Y. Tsunoda, J. Phys. G **43**, 024009 (2016).
[23] C. Santamaria *et al.*, Phys. Rev. Lett. **115**, 192501 (2015).
[24] F. Nowacki, A. Poves, E. Caurier, and B. Bounthong, Phys. Rev. Lett. **117**, 272501 (2016).
[25] Z. Y. Xu *et al.*, Phys. Rev. Lett. **113**, 032505 (2014).
[26] K. Sieja and F. Nowacki, Phys. Rev. C **85**, 051301(R) (2012).
[27] Y. Tsunoda, T. Otsuka, N. Shimizu, M. Honma, and Y. Utsuno, Phys. Rev. C **89**, 031301(R) (2014).
[28] G. Hagen, G. R. Jansen, and T. Papenbrock, Phys. Rev. Lett. **117**, 172501 (2016).
[29] A. Welker *et al.*, following Letter, Phys. Rev. Lett. **119**, 192502 (2017).
[30] S. Franchoo, M. Huyse, K. Kruglov, Y. Kudryavtsev, W. F. Mueller, R. Raabe, I. Reusen, P. Van Duppen, J. Van Roosbroeck, L. Vermeeren, A. Wohr, and K. L. Kratz, B. Pfeiffer, and W. B. Walters, Phys. Rev. Lett. **81**, 3100 (1998).
[31] K. T. Flanagan *et al.*, Phys. Rev. Lett. **103**, 142501 (2009).
[32] N. A. Smirnova, A. De Maesschalck, A. Van Dyck, and K. Heyde, Phys. Rev. C **69**, 044306 (2004).
[33] K. Sieja and F. Nowacki, Phys. Rev. C **81**, 061303(R) (2010).
[34] P. G. Hansen and J. A. Tostevin, Annu. Rev. Nucl. Part. Sci. **53**, 219 (2003).
[35] B. Zeidman and J. A. Nolen, Phys. Rev. C **18**, 2122 (1978).
[36] P. Morfouace *et al.*, Phys. Rev. C **93**, 064308 (2016).
[37] P. Morfouace *et al.*, Phys. Lett. B **751**, 306 (2015).
[38] T. Kubo *et al.*, Prog. Theor. Exp. Phys. **2012**, 03C003 (2012).
[39] N. Fukuda, T. Kubo, T. Ohnishi, N. Inabe, H. Takeda, D. Kameda, and H. Suzuki, Nucl. Instrum. Methods Phys. Res., Sect. B **317**, 323 (2013).
[40] A. Obertelli *et al.*, Eur. Phys. J. A **50**, 8 (2014).
[41] S. Takeuchi, T. Motobayashi, Y. Togano, M. Matsushita, N. Aoi, K. Demichi, H. Hasegawa, and H. Murakami, Nucl. Instrum. Methods Phys. Res., Sect. A **763**, 596 (2014).
[42] H. Kumagai, A. Ozawa, N. Fukuda, K. Sümmerer, and I. Tanihata, Nucl. Instrum. Methods Phys. Res., Sect. A **470**, 562 (2001).
[43] S. Agostinelli *et al.*, Nucl. Instrum. Methods Phys. Res., Sect. A **506**, 250 (2003).
[44] Y. Shiga *et al.*, Phys. Rev. C **93**, 024320 (2016).
[45] E. Sahin *et al.*, Phys. Rev. Lett. **118**, 242502 (2017).
[46] U. Köster, N. J. Stone, K. T. Flanagan, J. R. Stone, V. N. Fedosseev, K. L. Kratz, B. A. Marsh, T. Materna, L. Mathieu, P. L. Molkanov, M. D. Seliverstov, O. Serot, A. M. Sjödin, and Y. M. Volkov, Phys. Rev. C **84**, 034320 (2011).
[47] C. Petrone, J. M. Daugas, G. S. Simpson, M. Stanoiu, C. Plaisir, T. Faul, C. Borcea, R. Borcea, L. Caceres, S. Calinescu, R. Chevrier, L. Gaudefroy, G. Georgiev, G. Gey, O. Kamalou, F. Negoita, F. Rotaru, O. Sorlin, and J. C. Thomas, Phys. Rev. C **94**, 024319 (2016).
[48] D. Verney, F. Ibrahim, C. Bourgeois, S. Essabaa, S. Gales, L. Gaudefroy, D. Guillemaud-Mueller, F. Hammache, C. Lau, F. LeBlanc, A. C. Mueller, O. Perru, F. Pougheon, B. Roussiere, J. Sauvage, and O. Sorlin, Phys. Rev. C **76**, 054312 (2007).
[49] B. Cheal *et al.*, Phys. Rev. Lett. **104**, 252502 (2010).
[50] I. Stefanescu *et al.*, Phys. Rev. Lett. **100**, 112502 (2008).
[51] C. Mazzocchi *et al.*, Phys. Lett. B **622**, 45 (2005).
[52] T. Wakasa, K. Ogata, and T. Noro, Prog. Part. Nucl. Phys. **96**, 32 (2017).
[53] K. Amos, P. J. Dortmans, H. V. von Geramb, S. Karataglidis, and J. Raynal, Adv. Nucl. Phys. **25**, 276 (2000).
[54] A. Bohr and B. R. Mottelson, *Nuclear Structure* (Benjamin, New York, 1969), Vol. I.